etadata, citation and similar papers at core.ac.uk

Accepted Manuscript

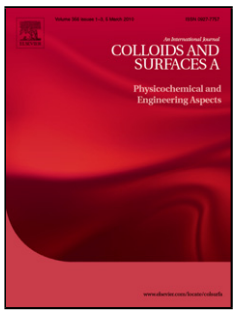

Title: Template synthesis of palladium nanotubes and their electrocatalytic properties

Author: Zhaopeng Li Hailong Lu Qun Li X.S. Zhao Peizhi Guo

PII: S0927-7757(14)00780-8
DOI: http://dx.doi.org/doi:10.1016/j.colsurfa.2014.10.010
Reference: COLSUA 19463

To appear in: *Colloids and Surfaces A: Physicochem. Eng. Aspects*

Received date: 2-7-2014
Revised date: 1-10-2014
Accepted date: 6-10-2014

Please cite this article as: Z. Li, H. Lu, Q. Li, X.S. Zhao, P. Guo, Template synthesis of palladium nanotubes and their electrocatalytic properties, *Colloids and Surfaces A: Physicochemical and Engineering Aspects* (2014), http://dx.doi.org/10.1016/j.colsurfa.2014.10.010

This is a PDF file of an unedited manuscript that has been accepted for publication. As a service to our customers we are providing this early version of the manuscript. The manuscript will undergo copyediting, typesetting, and review of the resulting proof before it is published in its final form. Please note that during the production process errors may be discovered which could affect the content, and all legal disclaimers that apply to the journal pertain.

Graphical Abstract

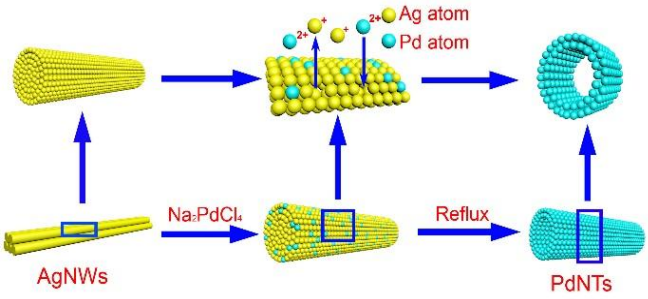

Accepted Manuscript

ACCEPTED MANUSCRIPT

Highlights

> Palladium nanotubes are synthesized by using silver nanowires as the template.

> Palladium nanotubes are polycrystalline composed of small palladium nanoparticles.

> Palladium nanotubes show the highest electrocatalytic activity for ethanol among used alcohols.

Accepted Manuscript

*Manuscript
ACCEPTED MANUSCRIPT

Template synthesis of palladium nanotubes and their electrocatalytic properties

Zhaopeng Li,[1,2] Hailong Lu,[1,2] Qun Li,[1,2] X. S. Zhao,[1,2,3] Peizhi Guo[1,2,*]

[1] State Key Laboratory Breeding Base of New Fiber Materials and Modern Textile, Collaborative Innovation Center for Marine Biomass Fibers, Materials and Textiles of Shandong Province, Qingdao University, Qingdao, 266071 P. R. China

[2] School of Chemical Science and Engineering, Qingdao University, Qingdao, 266071 P. R. China

[3] School of Chemical Engineering, The University of Queensland, St Lucia, QLD 4072, Australia

Corresponding author: Tel: +86 532 859 51290; Fax: +86 532 859 55529

E-mail address: guopz77@yahoo.com, pzguo@qdu.edu.cn

Accepted Manuscript

ACCEPTED MANUSCRIPT

Abstract: Palladium nanotubes were prepared by using silver nanowires as the template, which were prepared in a modified polyol reduction process. The morphology and structure of silver nanowires and palladium nanotubes were investigated by X-ray diffraction (XRD), scanning electron microscopy (SEM) and transmission electron microscopy (TEM). Electrochemical experimental data showed that palladium nanotubes displayed high electrocatalytic activity towards the electrooxidation of alcohols, especially for ethanol. The formation mechanism of palladium nanotubes as well as the relationship between their structure and electrocatalytic activity was discussed based on the experimental results.

Keywords: Palladium nanotubes; Silver nanowires; Template; Electrocatalysis

1. Introduction

As one type of the important power sources with high efficiency and no pollution [1,2], direct alcohol fuel cell (DAFC) has received great interest due to its potentially important applications in many fields, such as portable electronic devices and vehicles [3–5]. The choice of a suitable catalyst is essential to DAFC. Normally, platinum (Pt)-based electrocatalysts for DAFC can show excellent electrocatalytic activity for fuel molecules. However, high cost as well as the easy poison nature introduced by the CO-like intermediates of Pt-based electrocatalysts hinders their commercial development [6,7]. Thereafter, either the design of new Pt nanostructures with excellent electrochemical performances or the exploration of non-Pt electrocatalysts has attracted extensive interest [8–11]. Palladium can be considered as one of the

Accepted Manuscript

ACCEPTED MANUSCRIPT

important candidates for non-Pt catalyst systems due to its desirable performance toward the electrooxidation activity of small organic molecules, such as ethanol, methanol and formic acid [9–12].

Electrocatalytic activity of Pd nanostructures intensively depends on their size, shape and structure of the electrocatalysts [12–15]. So far, Pd nanostructures including nanocrystals, polyhedrons, nanosheets, nanorods and nanowires have been synthesized using various techniques, such as hydrothermal/solvothermal method, template and electrochemical methods [5,6,11–17]. For example, tetrahexahedral Pd nanocrystals with high-index facets are prepared by a simple electrochemical deposition method, which show excellent electrochemical activity toward formic acid and ethanol [12]. Hexagonal Pd nanosheets with plasmonic and high catalytic properties can be synthesized by a CO-confined growth method at low temperature [13]. Usually, Pd hollow structures can be synthesized from the spheric or tubular templates [17–25]. For example, Pd hollow sphere array can be prepared by electrodeposition of Pd on the SiO_2 spheres [16]. Pd nanotubes with tunable diameters were obtained using track etched polycarbonate templates by means of electrodeposition [18]. Vertical free-standing Pd nanotubes can be obtained based on the alumina membrane under an electric potential [22]. Pd nanotubes can also be synthesized by the one-dimensional template under a high temperature [23]. Pd/PANI/Pd sandwich nanotube array were prepared by using ZnO nanorod array as the template through a complicated procedure [24]. Despite recent progress, it is still a great challenge to synthesize Pd hollow nanostructures through a solution-phase

ACCEPTED MANUSCRIPT

synthetic strategy [24–26].

In this work, Pd nanotubes (PdNTs) were prepared by a simple displacement reaction using silver nanowires (AgNWs) as the template. The AgNW precursor can be synthesized by a modified polyol reduction process [27]. XRD results confirmed the successful synthesis of the AgNWs and corresponding PdNTs. TEM study demonstrated the formation of AgNWs and PdNTs and the selected area electron diffraction (SAED) pattern showed that PdNTs were polycrystalline. Electrochemical measurements showed that PdNTs displayed the highest electrocatalytic activity towards electrooxidation of ethanol among all the used alcohols.

2. Experiments

2.1 Materials

All reagents used in this article were of analytical grade and purchased from Sinopharm Chemical Reagent Company including palladium(II) chloride, silver nitrate, sodium chloride, glycerol, formic acid, sulfuric acid, methanol, ethanol, ethylene glycol (EG), acetone and polyvinyl pyrrolidone (PVP) (molar weight= 30 000). Double distilled water was used in the experiments except ultrapure water (18.2 MΩ•cm) for electrochemical measurements.

2.2 Synthesis of silver nanowires and palladium nanotubes

AgNWs were synthesized according to the literature [27]. Typically, PVP (0.586 g) was added into 20 mL glycerol in a 50 mL round bottle flask with tender stirring, which was dissolved thoroughly in one hour with the gentle heating. After the

Accepted Manuscript

ACCEPTED MANUSCRIPT

temperature dropped down to room temperature, silver nitrate (0.158 g) was added into the above solution under stirring. After several minutes, NaCl (5.9 mg) and H_2O (50 μL) were added into the flask. The flask was then heated under stirring and the solution temperature was raised from room temperature to 210°C within 20 min. The color of the solution turned from colorless to light brown, red-gray, and eventually dark-gray with the continuous increase of the synthetic time. When the temperature reached 210°C, the heating was stopped and the temperature dropped back to room temperature slowly. After that, water (60 mL) was added into the solution, and then the mixture was centrifuged at 4800 rpm. The as-obtained AgNWs was washed thoroughly by water for three times to remove the PVP residue. AgNWs were collected and dispersed into 3 mL water (~20 mg/mL).

For the synthesis of PdNTs, aqueous Na_2PdCl_4 solution was obtained first by mixing aqueous $PdCl_2$ and NaCl solutions. Stock solution of AgNWs (1 mL) was dispersed into water (200 mL) and refluxed in a three-neck round bottom flask (1000 mL). Upon reaching the reflux temperature, Na_2PdCl_4 solution (100 mL, 1.0 mM) was added dropwise through the injection tube over a period of 15 min. The reaction mixture was refluxed for 10 min and subsequently quenched in an ice bath. After quenching, the product was washed in a saturated sodium chloride solution, followed by washing with water and ethanol, and then dried in an oven at 60°C for 6 h.

2.3 Characterization

Powder X-ray diffraction patterns (XRD) were recorded on a Bruker D8 Advance X-ray diffractometer equipped with graphite monochromatized Cu Kα radiation

Accepted Manuscript

ACCEPTED MANUSCRIPT

(λ=0.15418 nm) from 10 to 80 degrees (2θ) using a solid detector. Scanning electron microscopy (SEM) images were taken with a JSM-2000F scanning electron microscope operated at 20 kV. Transmission electron microscopy (TEM) images were measured with a JEM-2000EX transmission electron microscope. Energy dispersive spectroscopy (EDS) results were obtained with a JEOL 2100-FEG transmission electron microscope.

All the electrochemical measurements were conducted on a CHI760D workstation in a three-electrode cell at room temperature with platinum foil as counter electrode. A saturated calomel electrode (SCE) for acidic solutions, or an Hg/HgO electrode for alkaline solutions, was used as the reference electrode. The working electrode was prepared using a glassy carbon electrode (GCE, 3 mm in diameter). Before electrochemical measurements, a mixture containing 1.0 mg of electrocatalyst and 1 mL of ethanol was ultrasonicated for 30 min to obtain a well-dispersed ink. A 10 μL portion of the catalyst ink was then transferred onto the surface of the GC E and dried under the air to obtain a catalyst thin film. Cyclic voltammetry (CV) of alcohol electrooxidation was recorded in certain potential windows with the electrolytic solutions of 1 M alcohol in 1 M KOH.

3. Results and Discussion

Fig. 1a shows the XRD pattern of the as-made AgNWs. Four strong diffraction peaks at 2θ degrees of 38.3, 44.5, 64.6 and 77.5 can be clearly observed, which can be well ascribed to the (111), (200), (220) and (311) planes of pure Ag (JCPDS card NO.

ACCEPTED MANUSCRIPT

87-0597) with cubic phase. The sharp diffraction peaks of the sample indicate that the crystalline size of Ag nanoparticles in the sample is large, which is about 43.1 nm calculated from the (111) peak in the XRD pattern according to the Scherrer equation. As depicted in Fig. 1b, the SEM image of the product confirms the formation of one-dimensional nanostructures, in which the length of AgNWs can be extended to several micrometers [27]. Furthermore, most of AgNWs have a diameter of less than 60 nm, which is in good agreement with that derived from the XRD pattern. Figs. 1c and 1d show the typical TEM images of a single AgNW. It can be seen that AgNWs have a highly uniform diameter with the sizes of about 60 nm. Based on the SAED pattern of a single AgNW (the inset in Fig. 1c), it can be concluded that AgNWs have well crystalline nature with bright diffraction spots observed in the pattren. The unique structure of AgNWs can be considered as an ideal template to synthesize Pd nanotubular structures by using a simple replacement reaction.

Fig. 2a shows the XRD pattern of the formed PdNTs by using AgNWs as the template. Five diffraction peaks at 2θ values of 39.8, 46.5, 64.8, 81.7 and 85.9 are obviously observed which can be indexed into the (111), (200), (220), (311) and (222) plane of cubic phase Pd (JCPDS card NO. 88-2335), respectively. Different from the peaks in the XRD pattern of AgNWs, the diffraction peaks of PdNTs are clearly broad, indicating the existence of small Pd nanocrystals in PdNTs. The average size of Pd nanocrystals is calculated to be about 10.7 nm according to the Scherrer equation [28,29] based on the (111) peak in Fig. 2a. Furthermore, no Ag impurity can be observed in the as-made PdNTs based on the XRD pattern of PdNTs. Fig. 2b shows

Accepted Manuscript

ACCEPTED MANUSCRIPT

the typical TEM image of the as-made PdNTs, in which tubular nanostructures with diameters of about 60 nm are observed. In the meantime, a small part of nanoparticles can also be obtained. Obvious diffraction circles can be observed from the SAED pattern of the PdNTs, as shown in the inset of Fig. 2b, in which some diffraction spots also appear. These should be attributed to the structural nature of the as-formed PdNTs, in which Pd nanocrystals are not inclined to form large well-crystalline tubular structures. The EDS spectrum of PdNTs also confirms the formation of palladium phase (Fig. 2c).

The formation mechanism of PdNTs was proposed based on the experimental results and previous reports [30–32], as illustrated in Fig. 3. It is noticeable that the as-synthesized AgNWs are well separated (Figs. 1b-d). When the Na_2PdCl_4 solution was added dropwise into aqueous AgNW suspensions, the reactions begin among the reagents. The standard electrode potential is 0.796 V for Ag^+ ion to Ag, 0.951 V for Pd^{2+} ion to Pd and 0.591 V for $[PdCl_4]^{2-}$ ion to Pd. Thereafter, it is suggested that AgNWs in aqueous solution would not directly react with $[PdCl_4]^{2-}$ ions, but Pd^{2+} ions [31], which were existed due to the coordination equilibrium between Na_2PdCl_4 and $PdCl_2$, as shown in Fig. 2. Pd atoms should be formed on the surface of AgNWs due to the displacement reaction between Pd^{2+} ions and Ag. With the increase of the refluxing time, tiny Pd nanocrystals were gradually obtained to form a loose shell-like structure around the AgNWs. During the synthetic process, the rapid diffusion of Pd^{2+} and as-formed Ag^+ ions [24,31] as well as the Kirkendall effect [30] that some Ag atoms diffused out of the newly formed Pd shell would accelerate the displacement

ACCEPTED MANUSCRIPT

reaction at the high synthetic temperature. It is proposed that tubular Pd nanostructures, not Pd nanowires, are formulated because Ag^+ ions and newly formed Pd atoms/nanoparticles continuously diffused across the shell with the expense of the AgNW template.

Fig. 4a shows the CV curve of the PdNTs-modified GCE in aqueous 1 M H_2SO_4 solution at the scan rate of 50 mV/s. Clearly, the CV curve of the modified electrode is rather different from that of the naked GCE. It shows the typical features of those reported Pd-modified electrodes [11, 33-35]. For example, the sharp change of current at -0.18 V (vs SCE) is attributed to the generation of H_2 from the electrolysis of H_2O. The peak at -0.06 V (vs SCE) is attributed to the adsorption/desorption of hydrogen in the surface of PdNTs. The peak at 0.37 V (vs SCE) is the reduction peak of produced palladium oxide [35]. The electrochemically active surface area of the PdNTs-modified GCE is calculated to be 0.066 cm^2 based on a frequently used electrochemical method according to the formula of Q (μC)/424 cm^2. Compared with recent results about Pd nanostructures [11,12,29], this surface area value should be ascribed to the unique structural nature of PdNTs.

To study the electrocatalytic activity of PdNTs, the PdNTs-modified GCEs were used as working electrode for electrooxidation of small fuel molecules. It is found that PdNTs show a relative high electrocatalytic activity towards alcohols and formic acid (Figs. 4b-d) [11,36,37]. As depicted in Fig. 4b, the mass activity (current density per mass of catalyst metal loaded) is 1000 mA/mg for the positive scan and 1025 mA/mg for the negative scan for electrooxidation of ethanol (Fig. 4b). For the electrooxidation

ACCEPTED MANUSCRIPT

of formic acid, the mass activities are 310 and 340 mA/mg for the positive and negative scan, respectively (Fig. 4c). The difference in the catalytic current densities for positive and negative scans in Fig. 4c may be caused by adsorption of intermediate product which produces in the HCOOH oxidation process and covers partial active points of PdNTs on the modified GCE [5,38]. These results also indicate that the electrocatalytic activity of PdNTs is higher than that of Pd nanoparticles with a large crystalline size [11,15,16], but smaller than that of very small Pd nanoparticles [29]. The electrocatalytic activity of PdNTs has also been investigated for the electrooxidation of other alcohols, as shown in Fig. 4d. It is noticeable that the variations of the catalytic current densities toward the electrooxidation of alcohols are in accord with the order of ethanol > glycol > glycerol > methanol while the on-set voltage values of oxidation peak during the electrocatalysis are gradually increased with this order. Based on these experimental data, it is suggest that the electrocatalytic activity towards alcohols of the modified GCE may possibly obey with the same order [3,39-41]. It should also be noted that the inset in Fig. 4b shows the relationship curve between the mass activity and cycle number of the PdNTs-modified GCE toward ethanol electrooxidation at the scan rate of 50 mV/s. Clearly, the mass activity can reach the highest value quickly within several cycles. Furthermore, the mass activity can still maintain more than 60% of original value after 200 cycles, indicating that PdNTs modified GCEs still exhibits a relatively high electrocatalytic activity.

4. Conclusion

ACCEPTED MANUSCRIPT

Pd nanotubes are synthesized by a simple displacement reaction using Ag nanowires as the template. Ag nanowires can be obtained easily by a modified polyol reduction process using glycerol as the solvent. Based on the experimental results, it is suggested that a thin film made of Pd nanocrystals would be formed first on the surface of the template and then Pd nanotubes are gradually formulated with the expense of Ag nanowires ultimately. Electrochemical experimental results show that Pd nanotubes display a high electrocatalytic activity toward the electrooxidation of alcohols, especially for ethanol. These results should be helpful to the design and synthesis of novel nanostructured Pd electrocatalysts with high electrocatalytic performances.

Acknowledgment

This work was financially supported by the National Key Project on Basic Research (No.2012CB722705), the National High Technology Research and Development Program of China (No.2012AA110407), and the National Natural Science Foundation of China (No.21143006 and U1232104).

References

[1] B. Steele, A. Heinzel, Materials for fuel-cell technologies**,** Nature 414 (2001) 345–352.

[2] H. Zhang, W. Zhou, Y. Du, P. Yang, C. Wang, One-step electrodeposition of platinum nanoflowers and their high efficient catalytic activity for methanol electro-oxidation, Electrochem. Commun. 12 (2010) 882–885.

Accepted Manuscript

ACCEPTED MANUSCRIPT

[3] R. Lu, Y.X. Jiang, B.W. Zhang, L.X. You, J.H. Li, S.G. Sun, Electrocatalytic oxidation of ethanol, Prog. Chem. 26 (2014) 727–736.

[4] R. Bashyam, P. Zelenay, A class of non-precious metal composite catalysts for fuel cells, Nature 443 (2006) 63–66.

[5] V. Mazumder, S.H. Sun, Oleylamine-mediated synthesis of Pd nanoparticles for catalytic formic acid oxidation, J. Am. Chem. Soc. 131 (2009) 4588–4589.

[6] R. Inguanta, S. Piazza, C. Sunseri, Synthesis of self-standing Pd nanowires via galvanic displacement deposition, Electrochem. Commun. 11 (2009) 1385–1388.

[7] Z. Liu, X. Zhang, L. Hong, Physical and electrochemical characterizations of nanostructured Pd/C and PdNi/C catalysts for methanol oxidation, Electrochem. Commun. 11 (2009) 925–928.

[8] F. Vigier, S. Rousseau, C. Coutanceau, J.M. Leger, C. Lamy, Electrocatalysis for the direct alcohol fuel, Top. Catal. 40 (2006) 111–121.

[9] K.H. Young, J. Nei, The current status of hydrogen storage alloy development for electrochemical applications, Materials 6 (2013) 4574–4608.

[10] M.H. Shao, K. Sasaki, R.R. Adzic, Pd−Fe nanoparticles as electrocatalysts for oxygen reduction, J. Am. Chem. Soc. 128 (2005) 3526–3527.

[11] P.Z. Guo, Z.B. Wei, W.N. Ye, W. Qin, Q.C. Wang, X.F. Guo, C.J. Lu, X.S. Zhao, Preparation and characterization of nanostructured Pd with high electrocatalytic activity, Colloids Surf. A: Physicochem. Eng. Asp. 395 (2012) 75–81.

[12] N. Tian, Z.Y. Zhou, S.G. Sun, Electrochemical preparation of Pd nanorods with high-index facets, Chem. Commun. 12 (2009) 1502–1504.

[13] X. Huang, S. Tang, X. Mu, Y. Dai, G.X. Chen, Z.Y. Zhou, F.X. Ruan, Z.L. Yang, N.F. Zheng, Freestanding palladium nanosheets with plasmonic and catalytic

ACCEPTED MANUSCRIPT

properties, Nat. Nanotechnol. 6 (2011) 28–32.

[14] M.J. Ren, J. Chen, Y. Li, H.F. Zhang, Z.Q. Zou, X.M. Li, H. Yang, Lattice contracted Pd-hollow nanocrystals: Synthesis, structure and electrocatalysis for formic acid oxidation, J. Power Sources 246 (2014) 32–38.

[15] Z.X. Liang, T.S. Zhao, J.B. Xu, L.D. Zhu, Mechanism study of the ethanol oxidation reaction on palladium in alkaline media, Electrochim. Acta 54 (2009) 2203–2208.

[16] L. Yang, Z.C. Li, X.F. Lu, Y. Tong, G.D. Nie, C. Wang, One-pot synthesis of Palladium hollow nanospheres and their enhanced electrocatalytic properties, ChemPlusChem 78 (2013) 522–527.

[17] L. Dai, L.P. Jiang, E.S. Abdel-Halim, J.J. Zhu, The fabrication of palladium hollow sphere array and application as highly as active electrocatalysts for the direct oxidation of ethanol, Electrochem. Commun. 13 (2011) 1525–1528.

[18] V. Badri, A.M. Hermann, Metal hydride batteries: Pd nanotube incorporation into the negative eleetrode, Int. J. Hydrogen Energy 25 (2000) 249–253.

[19] M. Steinhart, Z. Jia, A.K. Schaper, R.B. Wehrspohn, U. Gösele, J.H. Wendorff, Palladium nanotubes with tailored wall morphologies, Adv. Mater. 15 (2003) 706–709.

[20] C.G. Hu, X.G. Zhai, Y. Zhao, K. Bian, J. Zhang, L.T. Qu, H.M. Zhang, H.X. Luo, Small-sized PdCu nanocapsules on 3D graphene for high-performance ethanol oxidation, Nanoscale 6 (2014) 2768–2775.

[21] A. Wang, H. Xu, J. Feng, L. Ding, Y. Tong, G. Li, Design of Pd/PANI/Pd sandwich-structured nanotube array catalysts with special shape effects and synergistic effects for ethanol electrooxidation, J. Am. Chem. Soc. 135 (2013) 10703–10709.

Accepted Manuscript

ACCEPTED MANUSCRIPT

[22] L. Liu, S. Park, Direct formation of thin-walled palladium nanotubes in nanochannels under an electrical potential, Chem. Mater. 23 (2011) 1456–1460.

[23] S. Alia, K. Juong, T. Liu, K. Jensen, Y. Yan, Palladium and gold nanotubes as oxygen reduction reaction and alcohol oxidation reaction catalysts in base, ChemSusChem 7 (2014) 1739–1744.

[24] S. Kim, L. Liu, S. Cho, H. Jang, S. Park, Synthesis of bimetallic Pt/Pd nanotubes and their enhanced catalytic activity in methanol electro-oxidation, J. Mater. Chem. A 1 (2013) 15252–15257.

[25] M. Steinhart, R.B. Wehrspohn, U. Gösele, J.H. Wendorff, Nanotubes by template wetting: a modular assembly system, Angew. Chem. Int. Ed. 43 (2004) 1334–1344.

[26] M.A. Mahmoud, R. Narayanan, M.A. El-sayed, Enhancing colloidal metallic nanocatalysis: sharp edges and corners for solid nanoparticles and cage effect for hollow ones, Acc. Chem. Res. 46 (2013) 1795–1805.

[27] C. Yang, H.W. Gu, W. Lin, M.M. Yuen, C.P. Wong, Silver nanowires: From scalable synthesis to recyclable foldable electronics, Adv. Mater. 23 (2011) 3052–3056.

[28] C. Li, R. Sato, M. Kanehara, H.B. Zeng, Y.S. Bando, T. Teranishi, Controllable polyol synthesis of uniform palladium icosahedra: effect of twinned structure on deformation of crystalline Lattices, Angew. Chem. Int. Ed. 48 (2009) 6883 –6887.

[29] Q.C. Wang, Y.Q. Wang, P.Z. Guo, Q. Li, B.Y. Wang, Formic acid-assisted synthesis of palladium nanocrystals and their electrocatalytic properties, Langmuir, 30 (2014) 440.

[30] Y. Yin, R.M. Rioux, C.K. Erdonmez, S. Hughes, G.A. Somorjai,

ACCEPTED MANUSCRIPT

A.P. Alivisatos, Formation of hollow nanocrystals through the nanoscale Kirkendall effect, Science 304 (2004) 711–714.

[31] Y.G. Sun, B. Mayers, Y.N. Xia, Metal nanostructures with hollow interiors, Adv. Mater. 15 (2003) 641–646.

[32] J.T. Zhang, J.Z. Ma, L.L. Zhang, P.Z. Guo, J.W. Jiang, X.S. Zhao, Template synthesis of tubular ruthenium oxides for supercapacitor applications, J. Phy. Chem. C 114 (2010) 13608–13613.

[33] W.C. Li, T.J. Balk, Preparation and hydrogen absorption/desorption of nanoporous palladium thin films, Materials 2 (2009) 2496–2509.

[34] C. Li, R. Sato, M. Kanehara, H.B. Zeng, Y.S. Bando, T. Teranishi, Controllable polyol synthesis of uniform palladium icosahedra: effect of twinned structure on deformation of crystalline Lattices, Angew. Chem. Int. Ed. 48 (2009) 6883 –6887.

[35] C. Wang, B. Peng, H.N. Xie, H.X. Zhang, F.F. Shi, W.B. Cai, Facile fabrication of Pt, Pd and Pt-Pd alloy films on Si with tunable infrared internal reflection absorption and synergetic electrocatalysis, J. Phys. Chem. C 113 (2009) 13841–13846.

[36] R. Inguanta, S. Piazza, C. Sunseri, Synthesis of self-standing Pd nanowires via galvanic displacement deposition, Electrochem. Commun. 11 (2009) 1385–1388.

[37] Y. Chen, B. He, T. Huang, et al. Controlled synthesis of palladium icosahedra nanocrystals by reducing H_2PdCl_4 with tetraethylene glycol, Colloids Surf. A: Physicochem. Eng. Asp. 348 (2009) 145–150.

[38] N. Tian, Z.Y. Zhou, S.G. Sun, Y. Ding, Z.L. Wang, Synthesis of tetrahexahedral

Accepted Manuscript

ACCEPTED MANUSCRIPT

platinum nanocrystals with high-index facets and high electro-oxidation activity, Science 316 (2007) 732–735.

[39] Y. Holade, C. Morais, S. Arrii-Clacens, K. Servat, T.W. Napporn, K.B. Kokoh, New preparation of PdNi/C and PdAg/C nanocatalysts for glycerol electrooxidation in alkaline medium, Electrocatalysis 4 (2013) 167–178.

[40] Z.G. Qi, A. Kaufmn, Liquid-feed direct oxidation fuel cells using neat 2-propanol as fuel, J. Power, Sources 118 (2003) 54–60.

[41] J. Lin, J. Ren, N. Tian, Z. Zhou, S. Sun, In situ FTIR spectroscopic studies of ethylene glycol electrooxidation on Pd electrode in alkaline solution: The effects of concentration, Journal of Electroanalytical Chemistry 688 (2013) 165–171.

Accepted Manuscript

ACCEPTED MANUSCRIPT

Figure Captions:

Fig. 1. The XRD pattern (a), SEM image (b) and TEM images (c,d) of AgNWs, the inset in **Fig.** 1c is the SAED pattern of a single AgNW.

Fig. 2. The XRD pattern (a), TEM image (b) and EDS spectrum (c) of PdNTs. The inset in **Fig.** 2b is the SAED pattern of PdNTs.

Fig. 3. Schematic illustration of the formation mechanism of PdNTs.

Fig. 4. CV curve of PdNTs modified GC electrode in (a) 1 M H_2SO_4 solution, (b) in 1M CH_3CH_2OH + 1 M KOH solution, (c) in 0.5 M HCOOH + 0.5 M H_2SO_4 solution and (d) in 1M alcohols + 1 M KOH solution . The inset in **Fig.** 4b is variation of current densities with cyclic number associated with the electrocatalytic oxidation in 1 M CH_3CH_2OH + 1 M KOH solution.

Accepted Manuscript

ACCEPTED MANUSCRIPT

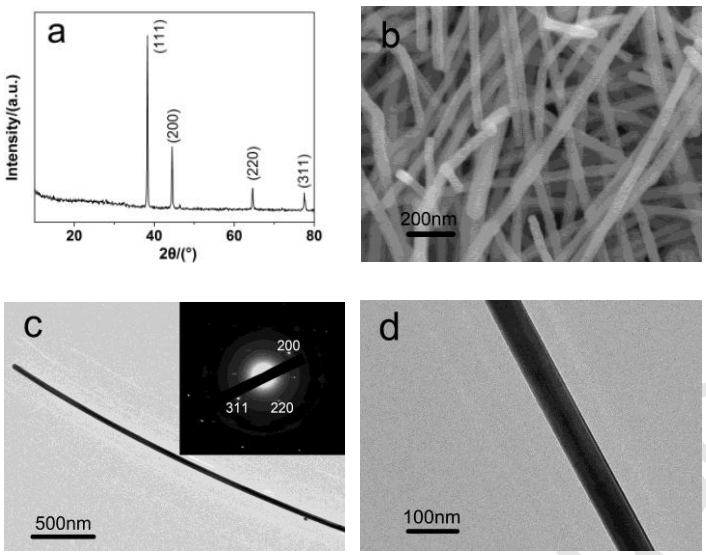

Fig. 1. The XRD pattern (a), SEM image (b) and TEM images (c,d) of AgNWs, the inset in **Fig.** 1c is the SAED pattern of a single AgNW.

Accepted Manuscript

ACCEPTED MANUSCRIPT

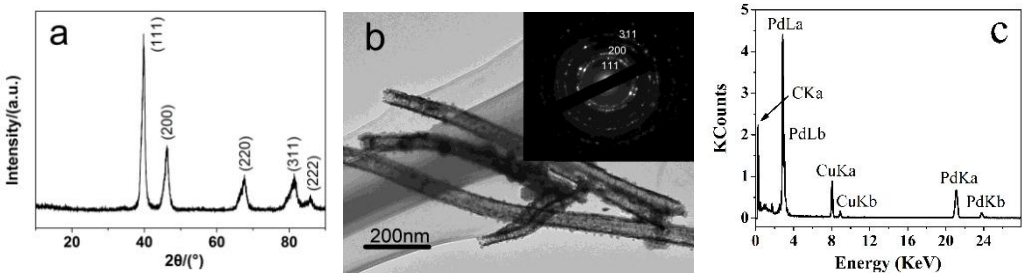

Fig. 2. The XRD pattern (a), TEM image (b) and EDS spectrum (c) of PdNTs. The inset in **Fig.** 2b is the SAED pattern of PdNTs.

Accepted Manuscript

ACCEPTED MANUSCRIPT

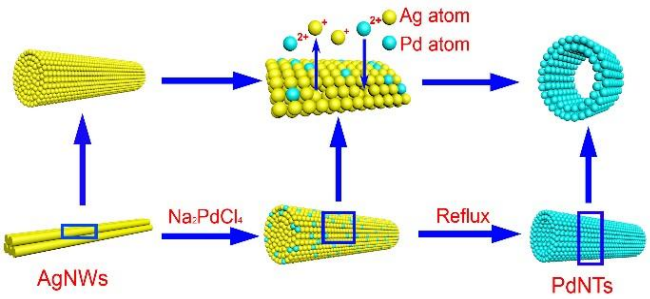

Fig. 3. Schematic illustration of the formation mechanism of PdNTs.

Accepted Manuscript

ACCEPTED MANUSCRIPT

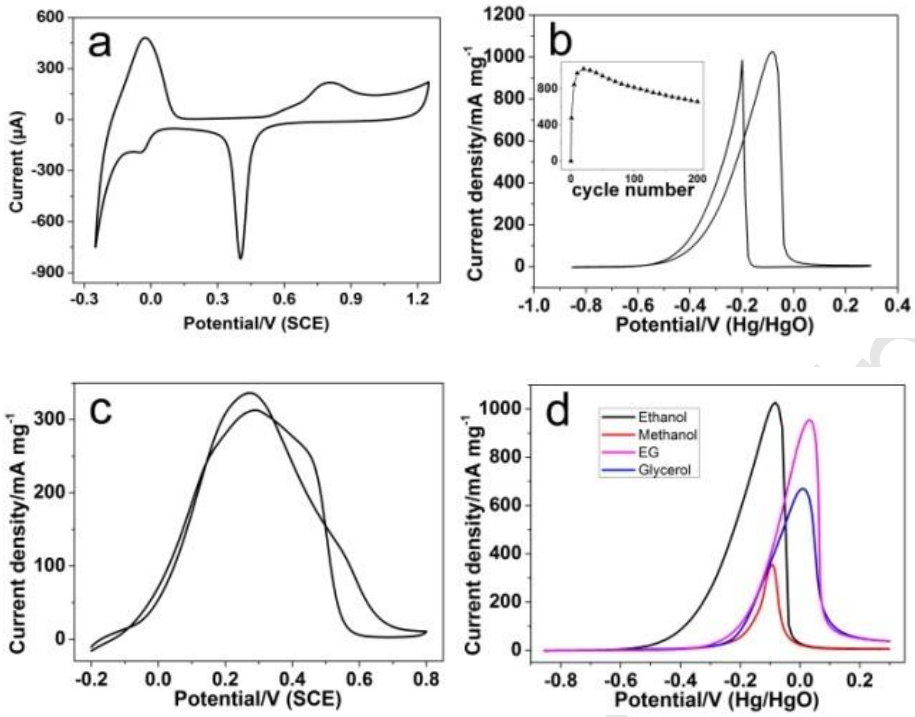

Fig. 4. CV curve of PdNTs modified GC electrodes in (a) 1 M H_2SO_4 solution, (b) in 1M CH_3CH_2OH + 1 M KOH solution, (c) in 0.5 M HCOOH + 0.5 M H_2SO_4 solution and (d) in 1M alcohols + 1 M KOH solution. The inset in **Fig.** 4b is variation of current densities with cyclic number associated with the electrocatalytic oxidation in 1 M CH_3CH_2OH + 1 M KOH solution.

Accepted Manuscript